

# A novel image based algorithm for interface level detection in a separation cell

Phanindra Jampana \* Sirish Shah \*\*

\* Department of Chemical Engineering, University of Alberta,  
Edmonton, Canada (e-mail: pjampana@ualberta.ca)

\*\* Department of Chemical Engineering, University of Alberta,  
Edmonton, Canada (e-mail: slshah@ualberta.ca)

---

**Abstract:** Controlling the interface between Bitumen-froth and Middlings in separation cells in the oil sands industry is important for economical and environmental reasons. Traditional sensors do not provide reliable measurements of this interface level and image based sensors are being used to alleviate this problem. Previous work in this area has focussed on separation cells with a single side-view glass. The current work describes a new image based algorithm for interface level detection and confidence estimation based on the concept of image differencing. The algorithm can be extended in a straight-forward manner to separation cells with arbitrary number of side-view glasses. Off-line and on-line results show that the algorithm accurately detects the interface level in normal process conditions and outputs correct confidence values in other situations with very low false positive and negative rates.

*Keywords:* Bitumen-froth Middlings interface, image sensors, image differencing

---

## 1. INTRODUCTION

The control of Bitumen-froth and Middlings interface using image based sensors has been approached previously (Jampana et al., 2008) via particle filtering techniques. Images obtained from a *side-view* glass camera are processed in real time for estimates of the interface level and its quality. These estimates are used subsequently for automatic control. A typical camera image from this setup is shown in Fig 1. For separation cells with multiple side-view glasses (Fig 2) the algorithm described there does not generalize in a straight forward manner. The current work describes an interface level detection algorithm based on image differencing which can be easily generalized to arbitrary number of side-view glasses.

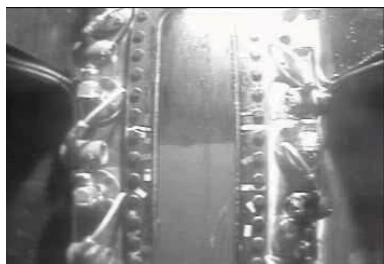


Fig. 1. Separation cell with single side view glass

The generalization property is achieved by computing a confidence estimate (in addition to the interface level estimate) for each side-view glass. This confidence estimate quantifies the chance of the presence of an interface. The final interface level estimate is obtained from the view

\* Financial support from NSERC, Matrikon, Suncor and iCORE in the form of the Industrial Research Chair(IRC) program at the University of Alberta is gratefully acknowledged.



Fig. 2. Separation cell with three side view glasses

glass with the highest quality. As confidence estimation is not entirely independent of the interface level estimation procedure, the interface level estimation procedure should facilitate the computation of quality values in an easy manner. The image differencing algorithm described in this paper is one such method.

The image differencing method is based on the idea that the *change* from any previous video frame to the current video frame is maximum near the current interface, though this maximum need not be unique. This change is detected here through (absolute) image differencing. To ensure that the maximum change occurs very close to the current interface, (absolute) image differences between the current and many previous frames are used. The sum image of all these differenced images has maximum values located close to the current interface level for ideal interface images, i.e. images which are completely free from noise. The proof of this fact is given in section 2.

In reality, interface images are seldom noise free. This leads us into estimating a quality value which reflects whether the current interface level estimate is purely a result of

noise. To compute the final confidence estimate however, the noise based quality value alone would not suffice. This is because abnormal changes might occur in the separation cell, which cannot be ascribed to noise alone and which do not necessarily imply the existence of a true interface. Fig 3 shows an example of such a change where the noise based quality described above might be high but the interface is spurious.

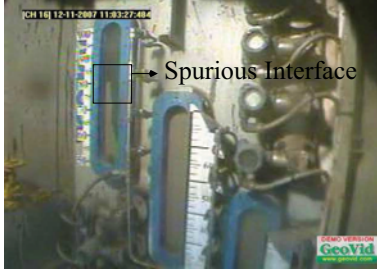


Fig. 3. Abnormal process condition resulting in a spurious interface

Therefore, apart from the noise based quality value, an edge quality is also estimated. This quality value quantifies the number of edges detected near the interface estimate. The edge detection method employed here is described in (Elder and Zucker, 1998). A combination of both these quality estimates suppresses most false negatives. In a few pathological cases however, both the noise based quality and the edge based quality can be high, even though the detected interface is spurious. To make the algorithm robust to these, a change based quality is estimated. The final confidence estimate is then based on the three values - noise based quality, edge based quality and change based quality.

The rest of the paper is organised as follows: Section 2 presents the image differencing based interface level detection algorithm in detail followed by section 3 which describes the confidence estimation procedure. Results are displayed in section 4 and section 5 gives the concluding remarks.

## 2. INTERFACE LEVEL DETECTION USING ABSOLUTE IMAGE DIFFERENCING

This section presents two results which describe the image differencing method for ideal images and also provide theoretical bounds for the interface level estimates obtained. The following notation is fixed first.

Let,

- (1)  $I_t$  represent the video frame obtained at time  $t$
- (2)  $D_{t_1, t_2} = I_{t_1} - I_{t_2}$ , be the difference of two images at times  $t_1$  and  $t_2$
- (3)  $AD_{t_1, t_2} = \text{abs}(I_{t_1} - I_{t_2})$ , be the absolute difference of two images at times  $t_1$  and  $t_2$
- (4)  $il(t)$  represent the interface level at time  $t$  (The interface level is always assumed to be on the Middlings side of the interface).
- (5)  $\mu_B(t), \mu_M(t)$  represent the average intensity values of pixels in the Bitumen-froth and Middlings regions at time  $t$ , respectively.
- (6)  $W$  and  $H$  represent the width and height of the interface image

- (7)  $C$  be the maximum change in the interface level between two successive video frames
- (8) The origin of images is always assumed to be at the top-left corner

*Lemma 1.* Consider a noise free interface having dynamics such that it remains horizontal at all times and having homogeneous pixel intensities in the Bitumen and Middlings regions. Let  $\{I_t, t = 0, 1, \dots\}$  be a sequence of completely noiseless images from such an interface such that  $\mu_B(0) = \mu_B(1) = \mu_B(2) = \dots$  and  $\mu_M(0) = \mu_M(1) = \mu_M(2) = \dots$ . If there is a change in the interface level in a time window  $[t_0, t_N]$  and if:-

$$J_N(i, j) = \sum_{k=0}^{N-1} AD_{t_N, t_k}(i, j),$$

$$\forall i \in \{0, 1, 2, \dots, H-1\},$$

$$j \in \{0, 1, 2, \dots, W-1\}$$

$$P_N(i) = \sum_{j=0}^{W-1} J_N(i, j), \forall i \in \{0, 1, 2, \dots, H-1\}$$

$$\hat{il}(t_N) = \inf_i (\arg \max_i P_N(i))$$

then,

- (1)  $P_N(i)$  is decreasing in  $i \in [\hat{il}(t_N), H-1]$  and increasing in  $i \in [0, \hat{il}(t_N)]$ ,
- (2)  $0 \leq il(t_N) - \hat{il}(t_N) \leq C$

In reality the interface is seldom horizontal. Lemma 2 guarantees similar bounds as above for the interface level estimate even for the more general case of non-horizontal interfaces:

*Lemma 2.* Consider the more general case of an interface having dynamics such that it can become non-horizontal. Let  $ip(t, v)$  for  $v \in [0, W-1]$  be the interface pixels at time  $t$ . If  $|ip(t, v) - ip(t, m)| < Q$ , for all  $v, m \in [0, W-1]$ ,  $t \in [t_0, t_N]$  and  $|ip(t_1, v) - ip(t_2, v)| < C$  whenever  $|t_1 - t_2| = 1$ ,  $v \in [0, W-1]$  and if there is a change in the interface in the time window  $[t_0, t_N]$  then it is true that  $-C \leq \hat{il}(t_N) - ip(t_N, v) \leq C + Q$  for some  $v \in [0, W-1]$ .

(Proof for both proofs are omitted due to a lack of space but are available from the authors). The above lemma shows that in the absence of noise and non-homogenities in images, the estimated interface level is close to the actual interface, especially if  $C$  and  $Q$  are small. However, when the images are corrupted by noise and other non-homogenities in pixel intensities, the estimated interface level might not be close to the actual interface. Hence a confidence value of the interface level estimate is computed.

## 3. CONFIDENCE ESTIMATION

The analysis above assumed that images obtained are completely noise free - an assumption that is never met in practice. Image noise is modelled to be additive, homogeneous and Gaussian with zero mean and variance  $\sigma^2$ .

In the presence of noise, it might no longer be true that  $\hat{il}(t_N)$  will lie close to an interface point as predicted by

Lemmas 1 and 2. This is because the images observed are only instantiations of a (two dimensional) random field, which is completely described only by the noise statistics, the interface level  $il(t_N)$  and the Middlings and Bitumen pixel intensities  $\mu_M(t), \mu_B(t)$ . Hence, each  $P_N(i)$  for  $i \in [0, H - 1]$  now has a probability distribution. In the case of a horizontal interface, given the noise distribution, the probability that is of interest is the following:-

$$P(P_N(il(t_N)) > \max_{|j-il(t_N)| > G} P_N(j))$$

The above probability quantifies the chance of obtaining an interface level estimate (by following the differencing method described before),  $\hat{il}(t_N)$ , which satisfies  $|\hat{il}(t_N) - il(t_N)| \leq G$ . This probability can be used as the confidence value but it cannot be determined, as  $il(t_N)$  cannot be known a priori.

As the theoretical confidence (the probability above) cannot be computed, a confidence estimate is obtained by heuristic methods. The confidence estimate is based on the following three quality values, which are explained subsequently:

- Noise based quality
- Edge based quality
- Change based quality

### 3.1 Noise based quality

Let  $TP(t, i, j)$  represent the true (expected) pixel value in the image at time  $t$  and at the location  $i, j$ . Then the observed value of each pixel  $I_t(i, j)$  can be written as  $TP(t, i, j) + Y(t, i, j)$ , where  $Y(t, i, j)$  is a random variable whose distribution is the same as the estimated noise distribution. Using this, the following can be derived:

$$\begin{aligned} P_N(i) - \sum_{j=0}^{W-1} \sum_{k=0}^{N-1} |Y(t_N, i, j) - Y(t_k, i, j)| \\ \leq \sum_{j=0}^{W-1} \sum_{k=0}^{N-1} |TP(t_N, i, j) - TP(t_k, i, j)| \\ \leq P_N(i) + \sum_{j=0}^{W-1} \sum_{k=0}^{N-1} |Y(t_N, i, j) - Y(t_k, i, j)| \end{aligned}$$

The above inequality gives loose bounds on the actual values,  $\sum_{j=0}^W \sum_{k=0}^{N-1} |TP(t_N, i, j) - TP(t_k, i, j)| \equiv M(i)$ , i.e., the values which would have resulted if the images are noise free. In practice, only one instance of  $P_N(i)$  is observed. From this value, the value of the corresponding instance of  $R_N(i) \equiv \sum_{j=0}^W \sum_{k=0}^{N-1} |Y(t_N, i, j) - Y(t_k, i, j)|$  cannot be computed. Therefore the bounds above cannot be determined exactly.

Given  $P_N(i) = \hat{P}_N(i)$ ,  $R_N(i)$  follows the conditional probability distribution given by  $P(R_N(i)|P_N(i) = \hat{P}_N(i))$ . Considering the instances ( $\hat{R}_N(i)$ ) of this distribution allows us to compute inequalities which are obeyed with a certain degree of probability. For example, if  $P_{R_N(i)|P_N(i)}(R_N(i) \leq \hat{R}_N(i)) = r(i)$ , then the inequalities

$$\hat{P}_N(i) - \hat{R}_N(i) \leq M(i) \leq \hat{P}_N(i) + \hat{R}_N(i)$$

are true with a probability of  $r(i)$ . If  $\hat{R}_N(i)$  are chosen such that  $r(i)$  are very high, then the inequalities are very likely to be satisfied. On the other hand, if the  $\hat{R}_N(i)$  are chosen such that  $r(i)$  are very low, it is very unlikely that the inequalities will be correct. Given a choice of  $\hat{R}_N(i)$ , the noise based quality can be defined as:

$$Q_{noise}(t_N) = \begin{cases} 0; & \text{if } \exists i, |i - \hat{il}(t_N)| > N_{TH}, \\ \hat{P}_N(i) + \hat{R}_N(i) > \\ \hat{P}_N(\hat{il}(t_N)) - \hat{R}_N(\hat{il}(t_N)) & \\ 1; & \text{otherwise} \end{cases}$$

This quality value penalizes the interface level estimates when the minimum bound of  $M(\hat{il}(t_N))$  is less than the maximum bound of  $M(i)$ , for  $i$  far away ( $N_{TH} > C$ ) from the current interface. In this case, the interface estimate is said to be obtained purely due to camera noise and other irregularities in the images.

As the conditional probability distribution cannot be estimated, the instance  $\hat{R}_N(i)$ , is chosen based on the unconditional one. The support of the unconditional distribution is a superset of the support of the conditional distribution. Hence, for high values of  $\hat{R}_N(i)$  (based on the unconditional distribution) the inequalities obtained will very likely be true. But high values of  $\hat{R}_N(i)$  make the bounds very loose and are not useful for noise based quality estimation as most quality estimates will be zero. On the other hand, for small values of  $\hat{R}_N(i)$ , the quality estimates might be high but the inequalities themselves are true only with a very small probability.

The problem is to obtain estimates  $\hat{R}_N(i)$ , for which the inequalities will be true with a high probability and are tight enough for use in noise based quality estimation. In the absence of any other information, the choice  $E(R_N(i)) = \hat{R}_N(i)$ , where  $E$  represents mathematical expectation can be considered a possible candidate. From basic probability and the properties of the Gaussian distribution, it can be computed that  $E(R_N(i)) = NW\sigma\sqrt{\frac{8}{\pi}}$ .

The accuracy of the noise based quality estimates  $Q_{noise}(t_N)$ , obtained by the choice  $\hat{R}_N(i) = E(R_N(i))$  depends on the absolute difference of average pixel intensities  $|\mu_B(t_N) - \mu_M(t_N)|$ , the size of the images and the noise standard deviation  $\sigma$ . Based on this dependence, false positive and false negative error rates for the noise based quality are estimated.

When  $\sigma$  is small and  $|\mu_B(t_N) - \mu_M(t_N)|$  is high, the false positive rate is approximately 0 – 2%, which is small as expected. This rate increases with an increase in  $\sigma$  but decreases with an increase in  $|\mu_B(t_N) - \mu_M(t_N)|$ . The ratio  $\frac{|\mu_B(t_N) - \mu_M(t_N)|}{\sigma}$  can be considered as an upper bound on the Signal to Noise ratio (SNR). If  $\frac{|\mu_B(t_N) - \mu_M(t_N)|}{\sigma} = 10$ , the false positive error rate is 7 – 8% on an average.

For computing the false negative error rates, random interface images, which do not contain an interface are created. As these images do not contain any interface the percentage of time  $Q_{noise}(t_N) = 1$  is considered an estimate of the false negative error rate. In a simulation

study using the same parameters as above (except that  $\mu_B(t_N) = \mu_M(t_N)$ ), it has been found that there were no false negatives. As other type of examples cannot be readily created to study the false positive and negative error rates, they are estimated on real videos collected from a plant site. These are presented in Section 4.

### 3.2 Edge based quality

Noise based quality alone is not sufficient for estimating confidence. This is due to the fact that false negatives result when abnormal changes occur inside the separation cell (scenarios as shown in Fig 3) which cannot be explained by noise alone. Hence, an additional edge detection algorithm is used to aid in the estimation of the confidence.

The motivation for using edge detection to estimate a quality value is that the available information in images would be utilised in a very efficient manner as the edge based algorithm captures information which cannot be obtained by image differencing. Given only the difference images  $I(t) - I(s)$  for  $s < t$ , it is impossible to recover the edge map of  $I(t)$  and similarly given only the edge map of  $I(t)$ , it is impossible to estimate the difference images except in a few pathological cases. Using the image differencing and the edge detection algorithms simultaneously most false negatives (high confidence values when the interface level estimates are wrong), can be avoided.

The algorithm described in (Elder and Zucker, 1998) is used here with the already estimated variance  $\sigma^2$  of the Gaussian noise distribution. The advantage of this particular edge detection algorithm over standard algorithms (Sobel, Canny etc.) is its ability to detect edges over a large blur scale and contrast. The Bitumen-Middlings interface tends to become fuzzy when the percent of sand in the oil sands ore is high. The chosen algorithm can detect edges under these situations and hence is suitable for the purpose. Another reason for the choice is that spurious edges that occur due to sensor noise are minimised because of statistical bound checking based on the sensor noise variance in the algorithm. This increases the efficiency of the edge based quality.

A simple heuristic based on the number of edge points in a predefined window near the detected interface level is used to estimate the edge based quality. If  $EI$  is the edge map returned by the edge detection algorithm, and if  $nedges$  represent the number of edges in a predefined window near the detected interface level and  $E_{TH}$  is a given threshold then the edge based quality is defined as:

$$Q_{edge}(t_N) = \begin{cases} 0; & nedges < E_{TH} \\ 1; & \text{otherwise} \end{cases}$$

### 3.3 Change based quality

The edge detection algorithm, in most cases does not produce the exact edge map,  $EI$ . When spurious edges are detected (due to shadows, lighting glare etc.), the edge based quality might be high even when the interface level estimate is not correct. If the noise variance is under estimated, the noise based quality would also be high resulting in a wrong estimate of the interface level. False negatives in interface level detection can have an

undesired effect on the overall process as the controller takes immediate corrective action based on these false readings.

To make the algorithm robust to such cases a quality based on the percent change near the interface is estimated. The change based quality analyzes the instance of  $P_N$  observed,  $\hat{P}_N$ . An example  $\hat{P}_N$  (for a normal interface image sequence) is shown in Fig 4.

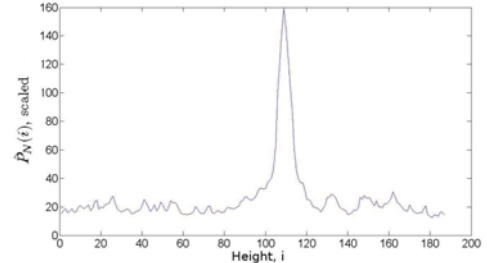


Fig. 4. An example of the profile,  $P_N$  obtained by the image differencing method

For a normal interface, based on test videos, the average and minimum values of  $\hat{P}_N$  have been observed to be close to each other as shown in the figure above. The maximum value of  $P_N$ ,  $\hat{P}_N(\hat{il}(t_N))$ , is in general high compared to both these values. Based on this, the change based quality is defined simply as:

$$Q_{change}(t_N) = \begin{cases} 0; & \frac{\max(\hat{P}_N) - avg(\hat{P}_N)}{\max(\hat{P}_N) - ((1 - \epsilon) \min(\hat{P}_N))} < C_{TH} \\ 1; & \text{otherwise} \end{cases}$$

Here,  $0 < \epsilon \approx 10^{-2} \ll \min(\hat{P}_N)$ . The change based quality value would be high when the average value of  $\hat{P}_N$  is close to the minimum value of  $\hat{P}_N$ . When the average is close to the maximum this quality value would be small.

The thresholds  $N_{TH}$ ,  $E_{TH}$ ,  $C_{TH}$  and  $N$  determine the performance of the final algorithm. The value of  $E_{TH}$  is chosen as a percentage of the width of the image  $W$  and the value of  $C_{TH} \in [0, 1]$ . Hence both these thresholds are relative in nature. The value of  $N_{TH}$  is chosen based on the dynamics of the interface. Based on the three quality values, the final confidence is defined as

$$il_{conf}(t_N) = \begin{cases} 1; & Q_{noise}(t_N) = 1, \\ & Q_{edge}(t_N) = 1, \\ & Q_{change}(t_N) = 1 \\ 0; & \text{otherwise} \end{cases}$$

## 4. RESULTS

### 4.1 Off-line results

The algorithm is first tested off-line on three videos recorded at the Suncor Energy Inc. plant site located at Fort McMurray, Alberta, Canada. The first video contained only one side view glass whereas the other two were equipped with three side view glasses. In the first video (Fig 5a) the view glass was wider and the interface was always present inside it. There was also significant lighting

glare present on the top of the glass window. The other two videos had considerably smaller view glasses. In one of these two videos (Fig 5c), the interface was only present in two of the three view glasses. In the other video (Fig 5b), spurious changes occurred (due to Bitumen sticking on the inside) in one of the glasses initially and the interface reappeared at the end.

The original videos were from colour cameras and for the purpose of analysis, they were converted to grayscale by averaging across all the three (RGB) colour channels. For single side view glass, the algorithm as described in the sections before can be applied directly. Whereas, in the case of three view glasses, the algorithm is extended in a straightforward manner. Each glass window is analysed separately and finally the window with the highest confidence value is chosen along with its interface level estimate. In cases where the interface is present in two or more glasses, more than one window can have a high confidence value. In such situations, the final interface level is chosen at random from these glasses, as all of the interface level estimates refer to the same interface.

In all the videos the same parameters,  $N = 100$ ,  $N_{TH} = 30$  pixels,  $E_{TH} = \frac{W}{4}$ ,  $C_{TH} = 0.75$  were used. Fig 6a shows the true and the estimated interface level values for the video with a single side view glass ( $H = 188$  pixels,  $W = 61$  pixels). It can be seen that the estimated value is very close to the actual value. The average absolute error was calculated to be approximately two pixels. This corresponds to an average error of less than one percent with respect to the height of the view glass. The confidence estimate was equal to one throughout (except at one frame where the edge based quality was zero). Noise standard deviation was estimated to be  $\sigma = 1.0$  pixels and  $|\mu_B(t_N) - \mu_N(t_N)| = 21.9$  intensity units. The corresponding false positive has been estimated to be zero which explains the fact that the noise based quality was equal to one throughout. Edge based quality was also high because the interface was clear and easily detectable by the edge detection algorithm. The change based quality was one throughout.

For the video with three side view glasses shown in Fig 5c, the results obtained are shown in Fig 6b. Note that in this case, the interface level estimate corresponds to the view glass with the highest confidence value. The average absolute error was calculated to be three pixels approximately, which corresponds to an average error of less than one percent with respect to the height of the view glass, as before. The confidence estimate was equal to one at all times except for three frames. The noise based quality was equal to one throughout but the edge based quality was zero at these three frames owing to significant fuzziness in the interface (not shown here). The change based quality was one throughout as before.

Finally, the video shown in Fig 5b is split into two segments. In the first part, the interface was either spurious or not present in the view glass. For this segment of the video the false negative rate obtained was equal to zero, i.e. the confidence value was identically zero all the time. Fig 6c shows the estimated and the actual interface level for the second part of the video, when the interface reappeared in the view glass. The average absolute difference was equal

to three pixels which corresponds to an error of less than one percent with respect to the height of the view glasses. The false positive rate during this time was estimated to be 10%, due to zero edge based quality during those frames. The high false positive rate in this video can be attributed to following:-

- Loss of resolution from the original to the recorded video resulting in a poor quality of the video
- Highly fuzzy interfaces occur due to a high fines situation – too many sand particles in the Bitumen-froth

The false positive rate can be minimized by employing a simple filtering rule. In the industry, a single occurrence of a confidence value of zero triggers an alarm for operator intervention. As the confidence value is susceptible to sudden changes in the fuzziness of the interface it is reasonable to wait until the confidence value stabilizes. Hence, instead of signalling an alarm for a single occurrence, alarm is only signalled when the confidence value is zero for a sustained period of time ( $\tau \approx 5s$ ). The interface level estimate used for control during this phase is the most recent estimate with a confidence value of one. This simple filtering rule has been observed to increase the efficiency of the algorithm.

#### 4.2 On-line results

The algorithm described in this paper has been implemented on two separation cells (previously shown in Fig 5b and Fig 5c) at Plant 86, Suncor Energy Inc., Fort McMurray, Alberta, Canada. A frame grabber card is used to transfer the images from the analog cameras to the PC. Software has been built in the C programming language based mainly on the Intel OpenCV library for image manipulation.

Fig 7a compares the true and estimated interface level values for the separation cell shown in Fig 5b. In this plot, hourly data is collected at random times and stitched together for the final result. A total of eight hours of data is used for comparison. On this data set, the average absolute error (in percentage) was calculated to be four percent. Similarly, Fig 7b compares the true and estimated interface level values for the separation cell shown in Fig 5c. The average absolute error was equal to three percent of the total height of the view glasses. These results suggest that the estimates from the vision sensor very closely reflect the true interface level values.

## 5. CONCLUSIONS

This work has presented a novel image differencing method for Bitumen-froth and Middlings interface level detection. It has been shown that in the case of noiseless images the estimation error is bounded. For nominal values of the dynamics of the separation cell, the bounds are very small.

When noise is present in the images, a confidence value which estimates the correctness of the detection is computed. The confidence value is based on a novel noise based quality estimate along with simple edge and change criterion. Analysis and results show that the final algorithm accurately detected the interface level and exhibited



Fig. 5. Interface levels in different separation cells

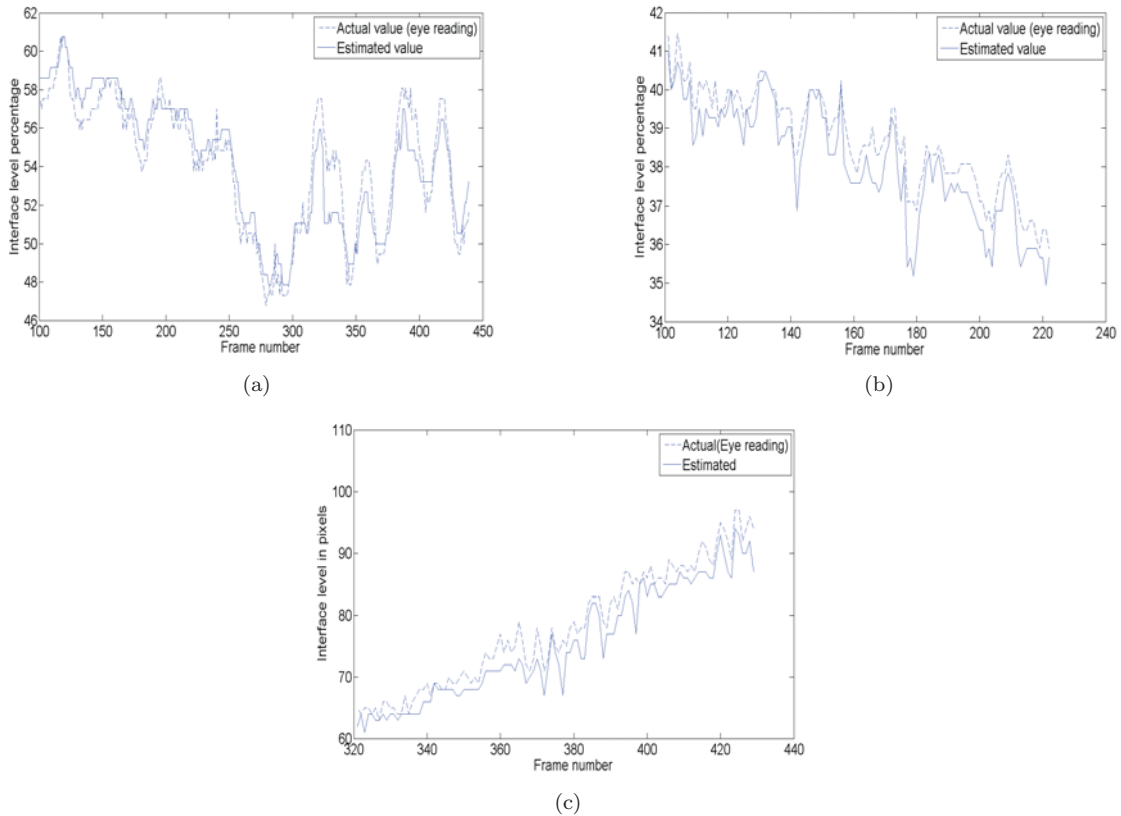
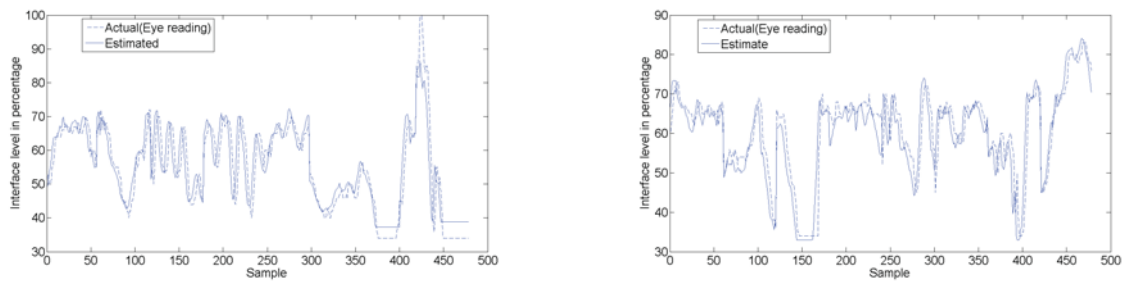


Fig. 6. True and estimated interface levels - Off-line results



(a) True and estimated interface levels for separation cell shown in Fig 5b

(b) True and estimated interface levels for separation cell shown in Fig 5c

Fig. 7. True and estimated interface levels - On-line results

very few false positive and negative error rates. The sensor has been installed at Suncor Energy, Inc, Fort McMurray, Canada and has been yielding highly satisfactory results.

REFERENCES

Elder and Zucker (1998). Local scale control for edge detection and blur estimation. *IEEE Transactions on*

*Pattern Analysis and Machine Intelligence*, 20(7), 699 – 716.  
 Jampana, P., Shah, S., and Kadali, R. (2008). Computer vision based interface level control in a separation cell. *IFAC world congress*.